

TECHNICAL  
REPORTS: DATA

10.1002/2017JA024446

## Key Points:

- Estimation of mesospheric neutral densities from meteor trail decay times observed by the Davis meteor radar
- The 9 and 6.75 day oscillations are observed in mesosphere neutral density over Antarctica in 2005 and 2006
- These periodic oscillations in density are associated with periodic changes in solar wind and recurrent geomagnetic activity

## Correspondence to:

I. M. Reid, and X. Xue,  
iain.reid@adelaide.edu.au;  
xuexh@ustc.edu.cn

## Citation:

Yi, W., I. M. Reid, X. Xue, J. P. Younger, A. J. Spargo, D. J. Murphy, T. Chen, and X. Dou (2017), First observation of mesospheric response to the solar wind high-speed streams, *J. Geophys. Res. Space Physics*, 122, 9080–9088, doi:10.1002/2017JA024446.

Received 14 JUN 2017

Accepted 3 AUG 2017

Accepted article online 7 AUG 2017

Published online 18 AUG 2017

## First observation of mesosphere response to the solar wind high-speed streams

Wen Yi<sup>1,2,3</sup> , Iain M. Reid<sup>3,4</sup> , Xianghui Xue<sup>1,2,5</sup> , Joel P. Younger<sup>3,4</sup> , Andrew J. Spargo<sup>3</sup>, Damian J. Murphy<sup>6</sup> , Tingdi Chen<sup>1,2</sup>, and Xiankang Dou<sup>1</sup>

<sup>1</sup>CAS Key Laboratory of Geospace Environment, Department of Geophysics and Planetary Sciences, University of Science and Technology of China, Hefei, China, <sup>2</sup>Mengcheng National Geophysical Observatory, School of Earth and Space Sciences, University of Science and Technology of China, Hefei, China, <sup>3</sup>School of Physical Sciences, University of Adelaide, Adelaide, South Australia, Australia, <sup>4</sup>ATRAD Pty Ltd, Thebarton, South Australia, Australia, <sup>5</sup>Synergetic Innovation Center of Quantum Information and Quantum Physics, University of Science and Technology of China, Hefei, China, <sup>6</sup>Australian Antarctic Division, Kingston, Tasmania, Australia

**Abstract** We present a first analysis of 9 and 6.75 day periodic oscillations observed in the neutral mesospheric density in 2005 and 2006. Mesospheric densities near 90 km are derived using data from the Davis meteor radar (68.5°S, 77.9°E; magnetic latitude, 74.6°S), Antarctica. Spectral analysis indicates that the pronounced periodicities of 9 and 6.75 days observed in the mesosphere densities are associated with variations in solar wind high-speed streams and recurrent geomagnetic activity. Neutral mesospheric winds and temperatures, simultaneously measured by the Davis meteor radar, also exhibit 9 and 6.75 day periodicities. A Morlet wavelet analysis shows that the time evolution of the 9 and 6.75 day oscillations in the neutral mesosphere densities and winds are similar to those in the solar wind and in planetary magnetic activity index,  $K_p$  in 2005 and 2006. These results demonstrate a direct coupling between Sun's corona (upper atmosphere) and the Earth's mesosphere.

## 1. Introduction

The middle and upper atmosphere are dominated by the effects of atmospheric waves, including planetary waves, tides, and gravity waves from below, as well as absorption of solar radiation, photochemical, photoionization, and geomagnetic forcing from above. Atmospheric motions at planetary wave periods (2–20 days) are known to propagate vertically from the lower to the upper atmosphere [e.g., Salby, 1984]. In addition to lower atmospheric sources of these waves, there appears to be a solar forcing of waves with planetary wave periods in the lower thermosphere. For example, Mlynczak *et al.* [2008] reported a 9 day periodic variation in the NO cooling in the thermosphere, and Lei *et al.* [2008a, 2008b] and Thayer *et al.* [2008] reported 5, 7, and 9 day subharmonics of the solar rotational period in thermosphere density at 400 km and suggested this was evidence of coupling between rotating solar coronal holes and the Earth's atmosphere. Subsequent studies have widely reported oscillations with periods of 5, 7, 9, and 13.5 day in the ionosphere [e.g., Lei *et al.*, 2008c, 2011; Tulasi Ram *et al.*, 2010] and the lower thermosphere [e.g., Crowley *et al.*, 2008; Chang *et al.*, 2009; Mlynczak *et al.*, 2010; Jiang *et al.*, 2014]. These observations were for the period of the declining phase of solar cycle 23, and the authors explained these periodic variations as being due to the modulation of periodic recurrent geomagnetic activity connected to corotating interaction regions (CIRs) in the solar wind. Lee *et al.* [2013, 2014] reported that oscillations with 7, 9, and 13.5 day periodicities are also observed in polar mesospheric summer echoes (PMSEs) at 80–90 km and indicated that these oscillations were also correlated with solar wind high-speed streams.

In this report, we estimate the daily mean neutral mesosphere densities at 90 km over the Antarctic using Davis meteor radar data from January 2005 to December 2006 and find oscillations with periodicities of 6.75 and 9 days in the neutral density. Further investigation indicates that these oscillations correspond to periodicities also observed in the solar wind speed and in geomagnetic activity. In addition, we also find oscillations with the same periodicities in mesospheric neutral temperatures and horizontal wind fields measured with the same radar. These new findings indicate that direct solar-terrestrial coupling is not confined to the thermosphere but also extends into the mesosphere.

## 2. Instruments and Data Sets

An all-sky meteor radar has been operated by the Australian Antarctic Division since 2005 at Davis Station ( $68.5^{\circ}\text{S}$ ,  $77.9^{\circ}\text{E}$ ; magnetic latitude,  $74.6^{\circ}\text{S}$ ), Antarctica. It operates at a frequency of 33 MHz with a peak power of 7.5 kW. It is an ATRAD meteor detection radar (MDR) and is essentially the same as that described by Holdsworth *et al.* [2004]. Data obtained by this radar from January 2005 to December 2006 were used in this study, because the 9 and 6.75 day periodicities are very strong in solar wind high-wind steams and recurrent geomagnetic activity in these two years [e.g., Lei *et al.*, 2008a; Thayer *et al.*, 2008]. There are two large data gaps in January 2005 (a 25 day gap) and February 2006 (a 20 day gap), and we interpolate over these data gaps using simultaneous data obtained by the Davis Stratospheric-Tropospheric (ST)/meteor radar [Reid *et al.*, 2006], after correcting for amplitude differences. The ST/meteor radar is operated at 55 MHz and is collocated with the 33 MHz Davis meteor radar. Further descriptions of these radars and their capabilities are described in detail by Holdsworth *et al.* [2006, 2008] and Younger *et al.* [2014].

The Microwave Limb Sounder (MLS) instrument is on board the Earth Observing System (EOS) Aura space-craft, which was launched in 2004. MLS observes atmospheric thermal microwave emissions in five spectral regions from 115 GHz to 2.5 THz. Temperatures are retrieved from bands near the  $\text{O}_2$  spectral lines at 118 GHz and 239 GHz [Schwartz *et al.*, 2008]. Aura MLS data within a radius of 300 km centered on the location of the Davis meteor radar were used in this study. The satellite temperatures taken on the same days as Davis meteor radar measurements were averaged to obtain daily mean temperatures. The daily mean MLS temperatures were used to develop the temperature gradient model described below and to compare to the Davis meteor radar temperatures.

The hourly averaged solar wind bulk speed observed by the Advanced Composition Explorer (ACE) satellite, the daily planetary magnetic activity index,  $K_p$ , and the daily solar activity proxy,  $F_{10.7}$  were also used in this study. The solar wind speed,  $K_p$  and  $F_{10.7}$  data were obtained from the Goddard Space Flight Centre/Space Physics Data Facility (GSFC/SPDF) OMNIWeb interface (<https://omniweb.gsfc.nasa.gov/ow.html>).

## 3. Data Analysis

In this study, we estimate the neutral mesosphere density from the meteor radar as follows.

First, we use the ambipolar diffusion gradient method to estimate the mesosphere temperature. An expression for temperature is given by Hocking [1999] as

$$T = S \left( 2 \frac{dT}{dz} + \frac{mg}{k} \right) \log_{10} e, \quad (1)$$

where  $T$  is the temperature at peak height,  $S$  is the slope of  $\log_{10} D$  as a function of height, and  $D$  is the ambipolar diffusion coefficient. The approach to the estimation of the slope  $S$  has been described in detail by Yi *et al.* [2016]. The expression  $dT/dz$  is the vertical temperature gradient, which we model by averaging the Aura MLS temperatures from an altitude of 83 km (at a pressure level of 0.0046 hPa) to an altitude of 87 km (at a pressure level of 0.0022 hPa) from 2005 to 2016, and then applying a harmonic fit of the annual, semiannual, terannual, and quarterly components to create a temperature gradient model.

The temperatures ( $T_{\text{Davis}}$ ) derived from the Davis meteor radar show larger fluctuations than the MLS temperatures ( $T_{\text{MLS}}$ ), but have a strong linear correlation with  $T_{\text{MLS}}$ , and the correlation coefficient between the two is 0.94. The linear fitted expression for the relationship is  $T_{\text{MLS}} = 0.76 T_{\text{Davis}} + 67.6$  K, and we use the simultaneous  $T_{\text{MLS}}$  to calibrate  $T_{\text{Davis}}$ .

The ambipolar diffusion coefficient  $D$  describes the rate at which plasma diffuses in a neutral background and is a function of atmospheric temperature,  $T$ , and atmospheric pressure,  $P$ , (or atmospheric density,  $\rho$ ) [see, e.g., Younger *et al.*, 2014] as given by

$$\rho = 2.23 \times 10^{-4} K_0 \frac{T}{D}, \quad (2)$$

where  $K_0$  is the ion zero-field mobility factor. Following Chilson *et al.* [1996], Cervera and Reid [2000], and Younger *et al.* [2014],  $K_0$  is assumed to be  $2.5 \times 10^{-4} \text{ m}^{-2} \text{ s}^{-1} \text{ V}^{-1}$ . Using the relation given by

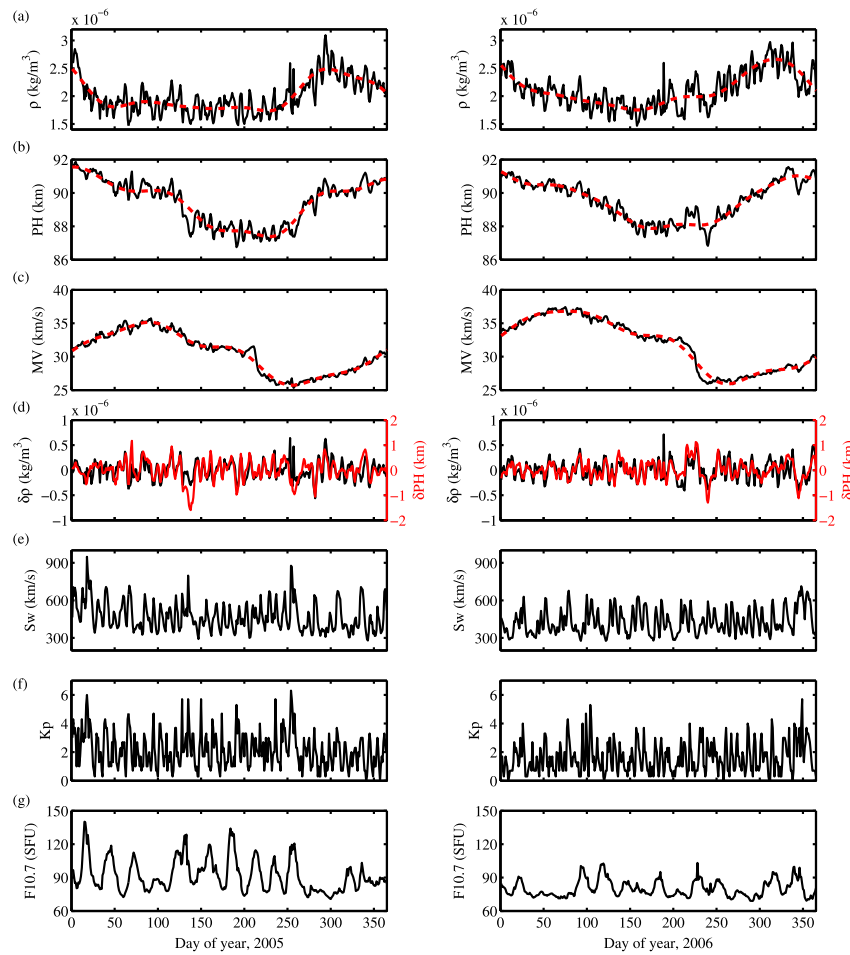


**Figure 1.** Variations of daily mean (a) Davis meteor radar density at 90 km ( $\rho$ ), (b) peak height (PH), (c) meteor velocity (MV), (d) residual of density ( $\delta\rho$ ) and peak height ( $\delta\text{PH}$ ) after the seasonal variations are removed, (e) solar wind velocity (SW), (f) magnetic activity index,  $K_p$ , and (g) solar EUV flux proxy,  $F_{10.7}$  for (left column) 2005 and (right column) 2006. The red dashed lines in Figures 1a–1c are harmonic fits consisting of annual, semiannual, terannual, and the quarterly components for the density and peak height, respectively.

equation (2), measurements of the temperature and ambipolar diffusion can be used to retrieve neutral mesospheric density [e.g., Takahashi *et al.*, 2002].

#### 4. Results

Figure 1a shows the variation of the daily mean density ( $\rho$ ) at 90 km in 2005 and 2006. The seasonal variations (red dashed lines in Figure 1a) of the Davis meteor radar densities mainly show an annual variation, with a maximum during late spring and a minimum during early winter. The annual changes of Davis meteor radar densities are approximately  $0.75 \times 10^{-6} \text{ kg/m}^3$  and  $0.91 \times 10^{-6} \text{ kg/m}^3$ , which translates to 37.8% and 43.1% of the yearly mean densities in 2005 and 2006, respectively.

Figure 1b shows the variations of the daily peak height (PH) in 2005 and 2006. The peak height of the meteor detection distribution can also serve as a proxy for the height of a constant neutral mesospheric density surface and can provide insight into planetary wave activity [e.g., Stober *et al.*, 2012]. Here we use the peak height to examine the neutral mesospheric density variabilities as well. However, as we can see from Figure 1b, the seasonal variations of density and peak height (red dashed lines in Figure 1b) are different, and the peak height shows an obvious maximum in summer, which the corresponding density estimates do not show. This suggests that the differences in the seasonal variations of density and peak height are caused by the annual variation of mean meteor velocity. This is evident as the daily mean meteor

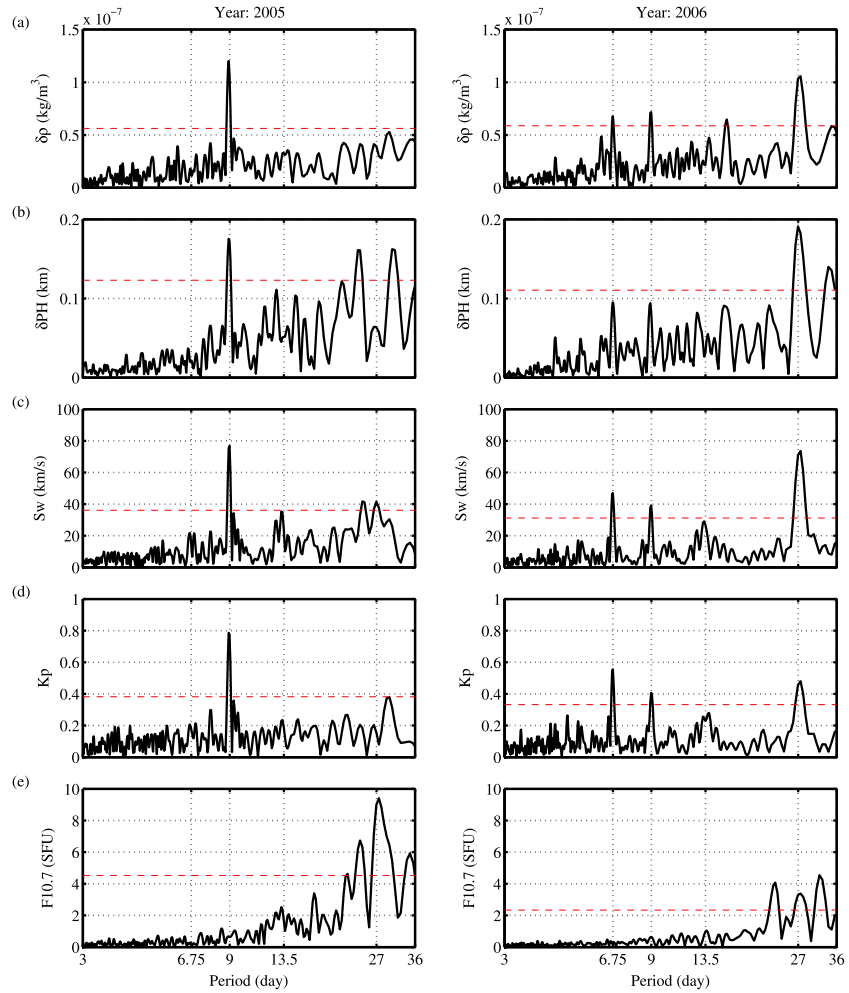


**Figure 2.** Lomb-Scargle periodograms of the residual from the (a) density and (b) peak height, and the (c) solar wind velocity, (d)  $K_p$ , and (e)  $F_{10.7}$  index for (left column) 2005 and (right column) 2006. The red dashed lines represent the 95% significance level.

velocities [see, e.g., Holdsworth *et al.*, 2007] shown in Figure 1c show the domination of the annual variation, with a maximum in early autumn (March) and a minimum in early spring (September). The faster meteors ablate over a shorter distance and generate meteor trails at larger altitudes; they are observed by meteor radars at higher altitudes. Similarly, slower meteors ablate over longer paths that extend to lower altitudes. Thus, the seasonal variations of peak height are a superposition of the effects of neutral mesospheric density and meteor velocity. We will present a more detailed discussion of this elsewhere.

To examine the short periodic variabilities in mesospheric density, we first remove the seasonal variations from the density and peak height. The residuals of density and peak height after seasonal variations are removed in 2005 and 2006 are presented in Figure 1d. The linear correlation coefficient between the residual of density and peak height is 0.75, and this indicates that the residual of density and peak height show similar characteristics to the wave variabilities in the neutral mesospheric density.

Figures 1e–1g show the variations of the daily solar wind velocity,  $K_p$  and  $F_{10.7}$ . The daily  $F_{10.7}$  is used as a proxy for the extreme ultraviolet (EUV) radiation and shows the domination of 27 day oscillations associated with solar rotation. However, the  $K_p$  and solar wind speed show significant oscillations with periods of less than 27 days.

Figure 2 shows the Lomb-Scargle periodograms [Lomb, 1976; Scargle, 1982] of the residual from density and peak height, solar wind speed,  $K_p$ , and  $F_{10.7}$ . Note that we only examine the 9 and 6.75 day periodicities in

this study, although periodicities of 13.5 and 27 days are also present in these measurements. This is because the 13.5 day periodicity is present but relatively weak in this 2 year period. In addition, the 13.5 and 27 day periodicities are observed in both geomagnetic activity and solar EUV radiation [e.g., *Mursula and Zieger, 1996*].

The periodograms of density in Figure 2a clearly show oscillations with periodicities of 9 days in 2005 and 6.75, and 9 days in 2006. The amplitudes of the 9 day oscillations of density are  $0.12 \times 10^{-6}$  kg/m<sup>3</sup> and  $0.072 \times 10^{-6}$  kg/m<sup>3</sup>, respectively, which translates to 6.3% and 3.4% of the yearly mean densities in 2005 and 2006. The amplitude of the 6.75 day periodicity in density is  $0.068 \times 10^{-6}$  kg/m<sup>3</sup>, which translates to 3.2% of the yearly mean density for 2006.

The Lomb-Scargle periodograms of peak height in Figure 2b show a similar periodic structure to the density, with a domination of the 9 day oscillation in 2005. The 6.75 and 9 day oscillations in 2006 are below the 95% confidence level, but peaks at these two periodicities are distinguishable. We also examined the daily mean meteor velocities in 2005 and 2006 and confirmed that there is no corresponding periodic change in the mean meteor velocities, which also can be seen in Figure 1c. This suggests that the 9 and 6.75 day oscillations in peak height are caused by similar periodic changes of mesospheric density.

As shown in Figures 2c and 2d, the Lomb-Scargle periodograms of solar wind speed and *Kp* index show similar periodicities and are dominated by a 9 day periodicity in 2005, and 6.75 and 9 day periodicities in 2006. These harmonic periodicities of 27 days arise from the average distribution of coronal holes in solar longitude. These occurrences can be sustained for several solar rotation periods during the declining phase of a solar cycle, when they are associated with CIRs and the frequent and periodical recurrent geomagnetic activity [Temmer et al., 2007; Lei et al., 2008a, 2011]. It is worth noting that the 9 day oscillation is the strongest feature in solar cycle 23, especially in the year of 2005, and the 13.5 day oscillation is weak in this solar cycle. Xu et al. [2015] compared the strength of the 9 and 13.5 day oscillations in thermospheric density from 1967 to 2007 and found that only during the declining phase of solar cycle 23 was the 9 day oscillation stronger than the 13.5 day oscillation. In addition to this, the 13.5 day oscillation was usually stronger than the 9 day oscillation.

The periodograms of the *F*<sub>10.7</sub> index in Figure 2e mainly show the 27 day oscillation in 2005 and 2006. Note that the peaks in density and peak height in the periodograms correspond well with those observed in the solar wind speed and geomagnetic activity and are quite distinct from those for the *F*<sub>10.7</sub> index. Thus, we can infer from the periodogram results in Figure 2 that the periodicities of 9 and 6.75 days in density and peak height are not associated with variations in the solar EUV flux.

To further examine the relationship between the 9 and 6.75 day oscillations in the neutral mesospheric density, solar wind speed, and geomagnetic activity, we apply a rectified Morlet wavelet analysis [see, e.g., Torrence and Compo, 1998; Liu et al., 2007] to the time series of the residual of neutral density and peak height, as well as that for the solar wind speed, *Kp* and *F*<sub>10.7</sub> index to observe the time evolution of the periodicities in 2005 and 2006. The corresponding Morlet wavelet power spectra for periods from 3 to 20 days in the time series are shown in Figure 3.

The wavelet spectral power of density in Figure 3a shows an obvious 9 day oscillation around days 50–170, days 180–220, and days 270–355 in 2005, and also short periods around days 85–105 and days 220–235 in 2006. The 6.75 day oscillation is the most prominent feature in 2006, which is consistent with the Lomb-Scargle results in Figure 2a and is present around days 50–60, days 120–130, days 150–200, days 250–300, and days 320–340.

As we can see from Figure 3b, the wavelet spectral power of peak height also shows a similar 9 day oscillation around days 50–70, days 100–170, days 180–220, and days 270–310 in 2005 and during a short period around days 220–235 in 2006. The 6.75 day oscillation in peak height is not as obvious in the density in 2006, but it is still clearly evident in some periods, such as around days 120–130 and days 150–200.

When we compare the wavelet spectral power of solar wind speed and *Kp* in Figures 3c and 3d, we find that the time evolution of the 9 and 6.75 day oscillation in the density and peak height perturbations matches well with those in both the solar wind speed and *Kp*. This indicates that the observed 9 and 6.75 day oscillations in the neutral mesospheric density are related to the variations of solar wind and geomagnetic activity. Finally, the wavelet spectra of *F*<sub>10.7</sub> in Figure 3e confirm again that the variations with periodicities of 9 and 6.75 days

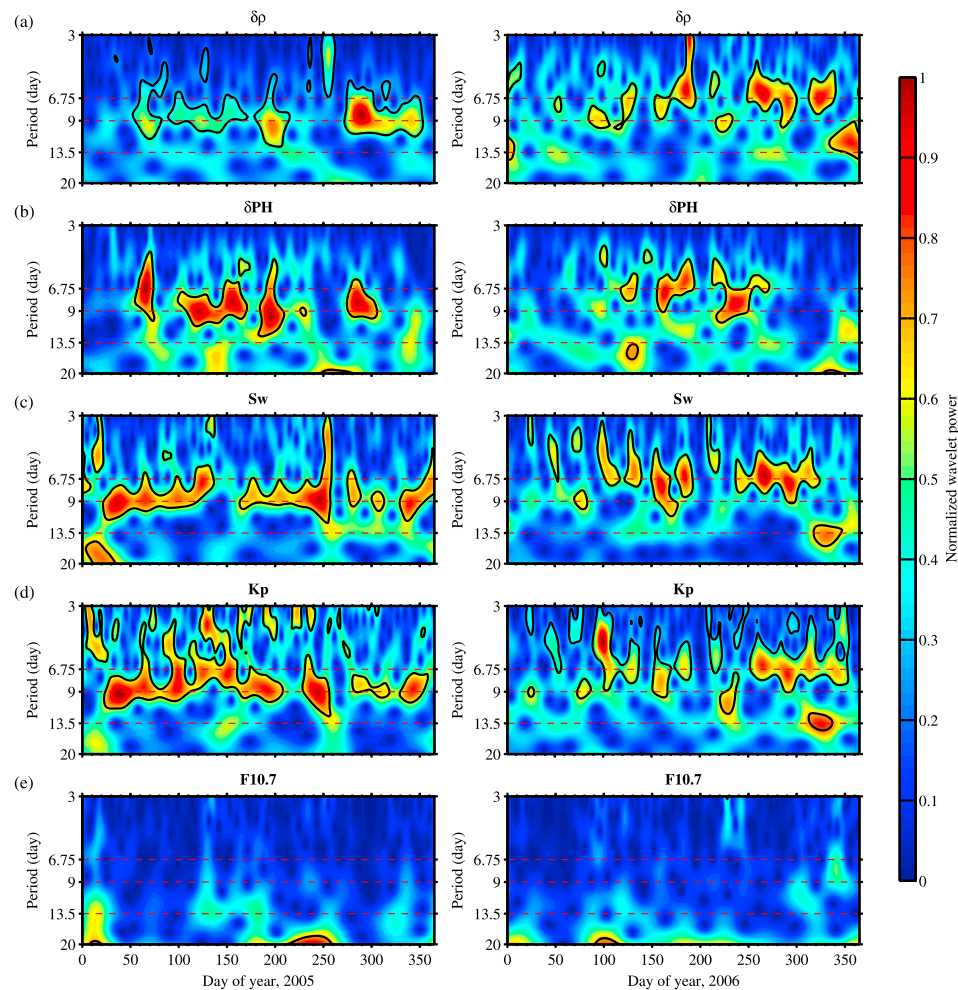


**Figure 3.** Wavelet power spectra of the time series of the (a) residual density, and (b) residual peak height, (c) solar wind velocity, (d)  $K_p$ , and (e)  $F_{10.7}$  index for (left column) 2005 and (right column) 2006. The black solid contours denote the regions of the wavelet spectrum above the 95% confidence level.

in density are not present in the  $F_{10.7}$  index during these 2 years, and so we can exclude solar EUV flux effects as a direct driver of these oscillations.

## 5. Discussion and Summary

The spectral analysis in Figures 2 and 3 performed on the Davis meteor radar density and peak height near 90 km indicates that oscillations with periodicities of 9 and 6.75 days in neutral mesospheric densities are present in 2005 and 2006 and are associated with solar wind high-speed streams and recurrent geomagnetic activity. However, a question arises as to whether the 6.75 and 9 day oscillation in the Davis meteor radar density truly reflects the actual mesospheric density variations. This is because the oscillations with periodicities of 9 and 6.75 days in density are also present in the daily ambipolar diffusion coefficients ( $D$ ) derived from the radar, and the estimation of density in this study mainly depends on the value of  $D$ . Given this, there are two possible explanations:

One possibility is that the geomagnetic field might influence the ambipolar diffusion process of the meteor trails plasma directly. Previous studies have indicated that the diffusion of meteor trails is dominated by ambipolar diffusion near 90 km [Chilson et al., 1996; Hocking et al., 1997]. However, because of the suppression by the geomagnetic field, the diffusion of meteoric plasma outward from the trail axis above 93 km becomes slower, and the geomagnetic field effect on ambipolar diffusion can no longer be ignored [Jones,

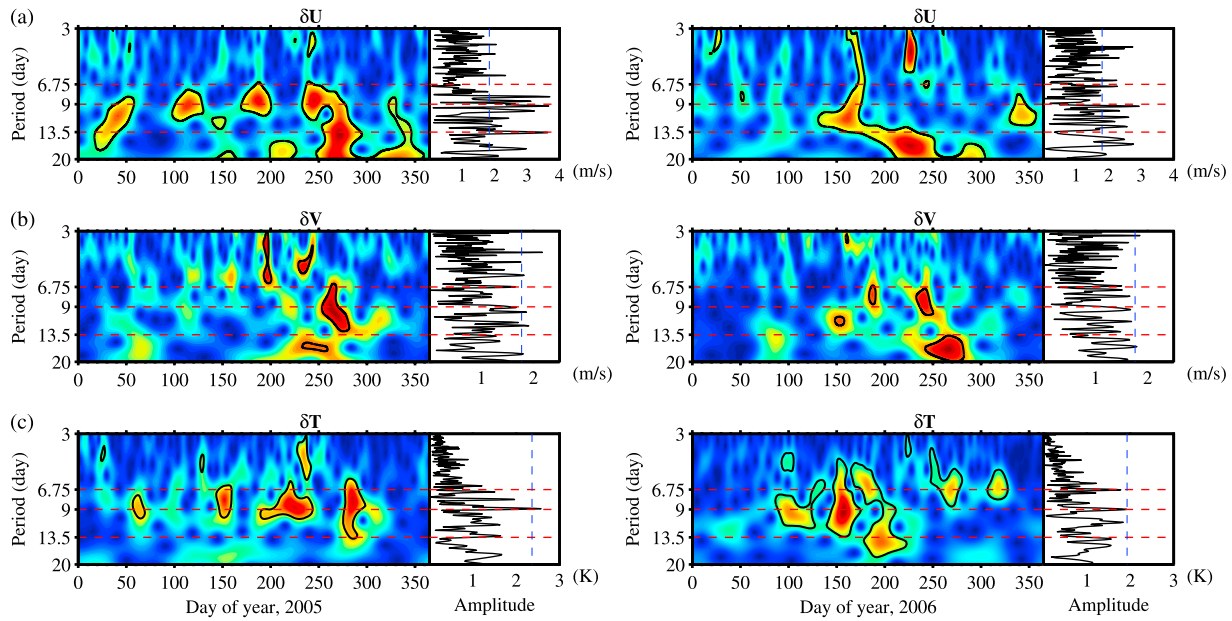


**Figure 4.** Wavelet power spectra of (a) residual zonal ( $\delta U$ ), (b) residual meridional ( $\delta V$ ) winds at 84 km, and (c) residual temperatures ( $\delta T$ ) near 90 km on the left-hand side, and the Lomb-Scargle periodograms for the zonal, meridional winds and temperatures on the right-hand side for reference for (left column) 2005 and (right column) 2006. The black solid contours denote the regions of the wavelet spectrum above 95% confidence level. The blue dashed lines represent the 95% significance level of the Lomb-Scargle periodogram.

1991; Cepelica *et al.*, 1998; Cervera and Reid, 2000; Hocking, 2004]. Whether or not the geomagnetic field effect on ambipolar diffusion could extend to near 90 km or even lower altitudes is still uncertain.

Another possibility is the 9 and 6.75 day oscillation in neutral mesospheric density and temperature might be directly forced by similar variations in recurrent geomagnetic activities, and then the ambipolar diffusion of meteor trails, which is controlled by neutral atmospheric density and temperature (as indicated by equation (2)), shows corresponding periodic responses.

In this study, we believe that the second explanation is much more convincing, and the reasons are as follows:

First, the 9 and 6.75 day oscillations are significant in the variations in the meteor peak detection height, and these match well with those observed in the solar wind and  $K_p$ . The peak height itself is mainly determined by the background neutral atmospheric density, and although there is a potential dependence on the meteor velocity, we found no such dependence between meteor detection peak height and daily mean meteor velocities in the present study.

Second, we also examined the horizontal wind fields observed by the meteor radar, and Figures 4a and 4b show the spectral analysis of zonal and meridional winds at 84 km. It can be seen clearly that the zonal winds in 2005 show a number of significant periodic oscillations with amplitude larger than 3.5 m/s, with a broad periodicity from 8 to 10 days, around days 30–50, days 100–130, days 170–200, days 230–260, and days 330–340. Note that the time of occurrence of these 9 day oscillations corresponds well with those shown in the solar wind and in  $K_p$ . It should be pointed out that the 9 day oscillations are present not just at 84 km but also in the region from 82 to 94 km in zonal wind in 2005. The 6.75 and 9 days periodicities are also present in the zonal and meridional wind in 2006 but are not as pronounced as in the zonal wind in 2005. The presence of these 9 and 6.75 day oscillations in the wind fields also suggests that the periodic oscillations in mesospheric density are real, rather than being an artifact of recurrent geomagnetic activity influencing the ambipolar diffusion coefficient.

As a reference, Lee *et al.* [2013] reported 7, 9, and 13 day periodic variations in PMSE count rates between 80 and 90 altitude at Esrange ( $67.8^\circ\text{N}$ ,  $20.4^\circ\text{E}$ ; magnetic latitude,  $64.75^\circ\text{N}$ ) in 2006 and 2008. Note that Lee *et al.* [2013] examined these periodic oscillations in MLS temperature over Esrange and found that these

oscillations were not present in MLS data. This has been confirmed in our study using the MLS temperature over Davis station (results not shown). However, here we show the presence of 9 day oscillation in neutral temperatures near 90 km derived from the Davis meteor radar in 2005 in Figure 4c, although the PMSE occurrence rates could be influenced directly by particle precipitation induced by auroral and other geomagnetic effects [Lee *et al.*, 2013].

The remaining interesting question is how periodic variations of solar wind and recurrent geomagnetic activity influence neutral mesospheric density and winds. Widely reported observations and simulations show that the responses to the periodic oscillations of recurrent geomagnetic activities are evident in the thermosphere and are stronger at high latitudes and altitudes than at low latitudes and altitudes [Lei *et al.*, 2008a, 2008b; Crowley *et al.*, 2008; Chang *et al.*, 2009; Mlynczak *et al.*, 2010; Qian *et al.*, 2010; Tulasi Ram *et al.*, 2010; Jiang *et al.*, 2014]. This is the first analysis of continuous observations of neutral mesospheric density over the Antarctic, and at a high geomagnetic latitude, and we might expect that periodic forcing by recurrent geomagnetic activity has stronger effects than at lower latitudes and could possibly penetrate down into the mesosphere.

The mechanism of these periodic oscillations in thermosphere density and temperature are considered to be driven by the periodic variation of Joule and particle heating [Lei *et al.*, 2008a, 2008b; Qian *et al.*, 2010; Jiang *et al.*, 2014]. But the simulations also show that the influence of Joule and particle heating caused by recurrent geomagnetic activity is confined to the lower thermosphere and does not penetrate down to the mesosphere [Qian *et al.*, 2010; Jiang *et al.*, 2014]. During strong magnetic storm induced by coronal mass ejection (CME), the enhanced joule and particle heating can penetrate down to the polar and middle-latitude mesosphere and lower thermosphere (MLT) region [Sinnhuber *et al.*, 2012; Yuan *et al.*, 2015]. However, in our study, we found the neutral mesospheric density to be sensitive to both the weak recurrent geomagnetic activity in 2006 and some strong magnetic storms in 2005. Our finding may demonstrate a previously undetected coupling mechanism between the mesosphere and magnetosphere-ionosphere-thermosphere (MIT) system. However, the actual mechanism of how the periodic variations in solar wind high-speed streams or recurrent geomagnetic activities can modulate neutral mesospheric densities and winds is still being investigated and will be reported in more detail in forthcoming papers.

#### Acknowledgments

This work is supported by the National Natural Science Foundation of China (41474129 and 41421063), the Chinese Academy of Sciences (KJCX2-EW-J01), the Youth Innovation Promotion Association of the Chinese Academy of Sciences (2011324), and the Fundamental Research Funds for the Central Universities and the China Scholarship Council. We also acknowledge support provided by the University of Adelaide and ATRAD Pty Ltd, and the provision of Davis meteor radar data by the Australian Antarctic Division. Operation of the Davis meteor radar was supported under AAS projects 2529 and 2668. We thank the NASA EOS Aura MLS team for providing free access to their data. The MATLAB wavelet analysis software was provided by C. Torrence and G. Compo and is available at URL <http://paos.colorado.edu/research/wavelets/software.html>, and a rectified wavelet analysis software was provided by Liu *et al.* [2007] and is available at URL <http://ocgweb.marine.usf.edu/~liu/wavelet.html>. Aura/MLS data are available from <http://disc.sci.gsfc.nasa.gov/Aura/data-holdings/MLS>. Meteor radar data are available from the University of Adelaide and the Australian Antarctic Division upon request. The involvement of I.M.R. and J.P.Y. was supported by ATRAD Pty Ltd.

In this study, we have reported for the first time, observation of 9 and 6.75 day oscillations in neutral mesospheric densities and shown that these periodic oscillations are linked to the recurrence of coronal holes and recurrent geomagnetic activities. These results provide new insight into solar-terrestrial coupling at mesospheric heights, as well as providing a new explanation of some “planetary wave period” oscillations in the mesosphere. While the results shown in this paper are confined to 2005 and 2006 and the Antarctic, these periodicities are strongly evident in meteor radar observations for the entire period from 2005 to 2008; moreover, we find a similar result for the Nippon/Norway Tromsø meteor radar [see, e.g., Hall *et al.*, 2006; Holmen *et al.*, 2016] (69.6°N, 19.2°E, magnetic latitude, 66.73°N) over the Arctic, and these will be reported in a following paper.

#### References

- Cepelka, Z., J. Borovicka, W. G. Elford, D. O. Revelle, R. L. Hawkes, V. Porubcan, and M. Simek (1998), Meteor phenomena and bodies, *Space Sci. Rev.*, 84, 327–471, doi:10.1023/A:1005069928850.
- Cervera, M. A., and I. M. Reid (2000), Comparison of atmospheric parameters derived from meteor observations with CIRA, *Radio Sci.*, 35, 833–843, doi:10.1029/1999RS002226.
- Chang, L. C., J. P. Thayer, J. Lei, and S. E. Palo (2009), Isolation of the global MLT thermal response to recurrent geomagnetic activity, *Geophys. Res. Lett.*, 36, L15813, doi:10.11029/12009GL039305.
- Chilson, P. B., P. Czechowsky, and G. Schmidt (1996), A comparison of ambipolar diffusion coefficients in meteor trains using VHF radar and UV lidar, *Geophys. Res. Lett.*, 23, 2745–2748, doi:10.1029/96GL02577.
- Crowley, G., A. Reynolds, J. P. Thayer, J. Lei, L. J. Paxton, A. B. Christensen, Y. Zhang, R. R. Meier, and D. J. Strickland (2008), Periodic modulations in thermospheric composition by solar wind high speed streams, *Geophys. Res. Lett.*, 35, L21106, doi:10.1029/2008GL035745.
- Hall, C. M., T. Aso, M. Tsutsumi, J. Höffner, F. Sigernes, and D. A. Holdsworth (2006), Neutral air temperatures at 90 km and 70°N and 78°N, *J. Geophys. Res.*, 111, D14105, doi:10.1029/2005JD006794.
- Hocking, W. K. (1999), Temperatures using radar-meteor decay times, *Geophys. Res. Lett.*, 26, 3297–3300, doi:10.1029/1999GL003618.
- Hocking, W. K. (2004), Radar meteor decay rate variability and atmospheric consequences, *Ann. Geophys.*, 22, 3805–3814, doi:10.5194/angeo-22-3805-2004.
- Hocking, W. K., T. Thayaparan, and J. Jones (1997), Meteor decay times and their use in determining a diagnostic mesospheric temperature-pressure parameter: Methodology and one year of data, *Geophys. Res. Lett.*, 24, 2977–2980, doi:10.1029/97GL03048.
- Holdsworth, D. A., I. M. Reid, and M. A. Cervera (2004), Buckland Park all-sky interferometric meteor radar, *Radio Sci.*, 39, RS5009, doi:10.1029/2003RS003014.

- Holdsworth, D. A., R. J. Morris, D. J. Murphy, I. M. Reid, G. B. Burns, and W. J. R. French (2006), Antarctic mesospheric temperature estimation using the Davis mesosphere-stratosphere-troposphere radar, *J. Geophys. Res.*, 111, D05108, doi:10.1029/2005JD006589.
- Holdsworth, D. A., W. G. Elford, R. A. Vincent, I. M. Reid, D. J. Murphy, and W. Singer (2007), All-sky interferometric meteor radar meteoroid speed estimation using the fresnel transform, *Ann. Geophys.*, 25, 385–398.
- Holdsworth, D. A., D. J. Murphy, I. M. Reid, and R. J. Morris (2008), Antarctic meteor observations using the Davis MST and meteor radars, *Adv. Space Res.*, 42(1), 143–154, doi:10.1016/j.asr.2007.02.037.
- Holmen, S. E., C. M. Hall, and M. Tsutsumi (2016), Neutral atmosphere temperature trends and variability at 90 km, 70°N, 19°E, 2003–2014, *Atmos. Chem. Phys.*, 16, 7853–7866.
- Jiang, G., W. Wang, J. Xu, J. Yue, A. G. Burns, J. Lei, M. Mlynczak, and J. M. Russell III (2014), Responses of the lower thermospheric temperature to the 9 day and 13.5 day oscillations of recurrent geomagnetic activity, *J. Geophys. Res. Space Physics*, 119, 4841–4859, doi:10.1002/2013JA019406.
- Jones, W. (1991), Theory of diffusion of meteor trains in the geomagnetic field, *Planet. Space Sci.*, 39(9), 1283–1288, doi:10.1016/0032-0633(91)90042-9.
- Lee, Y.-S., S. Kirkwood, G. G. Shepherd, Y.-S. Kwak, and K.-C. Kim (2013), Long-periodic strong radar echoes in the summer polar D region correlated with oscillations of high-speed solar wind streams, *Geophys. Res. Lett.*, 40, 4160–4164, doi:10.1002/grl.50821.
- Lee, Y.-S., S. Kirkwood, Y.-S. Kwak, K.-C. Kim, and G. G. Shepherd (2014), Polar summer mesospheric extreme horizontal drift speeds during interplanetary corotating interaction regions (CIRs) and high-speed solar wind streams: Coupling between the solar wind and the mesosphere, *J. Geophys. Res. Space Physics*, 119, 3883–3894, doi:10.1002/2014JA019790.
- Lei, J., J. P. Thayer, J. M. Forbes, E. K. Sutton, and R. S. Nerem (2008a), Rotating solar coronal holes and periodic modulation of the upper atmosphere, *Geophys. Res. Lett.*, 35, L10109, doi:10.1029/2008GL033875.
- Lei, J., J. P. Thayer, J. M. Forbes, E. K. Sutton, R. S. Nerem, M. Temmer, and A. M. Veronig (2008b), Global thermospheric density variations caused by high-speed solar wind streams during the declining phase of solar cycle 23, *J. Geophys. Res.*, 113, A11303, doi:10.1029/2008JA013433.
- Lei, J., J. P. Thayer, J. M. Forbes, Q. Wu, C. She, W. Wan, and W. Wang (2008c), Ionosphere response to solar wind high-speed streams, *Geophys. Res. Lett.*, 35, L19105, doi:10.1029/2008GL035208.
- Lei, J., J. P. Thayer, W. Wang, and R. L. McPherron (2011), Impact of CIR storms on thermosphere density variability during the solar minimum of 2008, *Sol. Phys.*, 274(1), 427–437, doi:10.1007/s11207-010-9563-y.
- Liu, Y., X. S. Liang, and R. H. Weisberg (2007), Rectification of the bias in the wavelet power spectrum, *J. Atmos. Ocean. Technol.*, 24(12), 2093–2102.
- Lomb, N. R. (1976), Least-squares frequency analysis of unequally spaced data, *Astrophys. Space Sci.*, 39, 447–462.
- Mlynczak, M. G., F. J. Martin-Torres, C. J. Mertens, B. T. Marshall, R. E. Thompson, J. U. Kozyra, E. E. Remsberg, L. L. Gordley, J. M. Russell III, and T. Woods (2008), Solar terrestrial coupling evidenced by periodic behavior in geomagnetic indexes and the infrared energy budget of the thermosphere, *Geophys. Res. Lett.*, 35, L05808, doi:10.1029/2007GL032620.
- Mlynczak, M. G., L. A. Hunt, J. U. Kozyra, and J. M. Russell III (2010), Short-term periodic features observed in the infrared cooling of the thermosphere and in solar and geomagnetic indexes from 2002 to 2009, *Proc. R. Soc. A*, doi:10.1098/rspa.2010.0077.
- Mursula, K., and B. Zieger (1996), The 13.5-day periodicity in the Sun, solar wind, and geomagnetic activity: The last three solar cycles, *J. Geophys. Res.*, 101(A12), 27,077–27,090, doi:10.1029/96JA02470.
- Qian, L., S. C. Solomon, and M. G. Mlynczak (2010), Model simulation of thermospheric response to recurrent geomagnetic forcing, *J. Geophys. Res.*, 115, A10301, doi:10.1029/2010JA015309.
- Reid, I. M., D. A. Holdsworth, R. J. Morris, D. J. Murphy, and R. A. Vincent (2006), Meteor observations using the Davis mesosphere-stratosphere-troposphere radar, *J. Geophys. Res.*, 111, A05305, doi:10.1029/2005JA011443.
- Salby, M. L. (1984), Survey of planetary-scale traveling waves: The state of theory and observations, *Rev. Geophys.*, 22(2), 209–236, doi:10.1029/RG022i002p00209.
- Scargle, J. D. (1982), Studies in astronomical time series analysis. II. Statistical aspects of spectral analysis of unevenly spaced data, *Astrophys. J.*, 263, 835–853.
- Schwartz, M. J., A. Lambert, G. L. Manney, W. G. Read, and N. J. Livesey (2008), Validation of the Aura Microwave Limb Sounder temperature and geopotential height measurements, *J. Geophys. Res.*, 113, D15S11, doi:10.1029/2007JD008783.
- Sinnhuber, M., H. Nieder, and N. Wieters (2012), Energetic particle precipitation and the chemistry of the mesosphere/lower thermosphere, *Surv. Geophys.*, 33, 1281–1334, doi:10.1007/s10712-012-9201-3.
- Stober, G., C. Jacobi, V. Matthias, P. Hoffmann, and M. Gerding (2012), Neutral air density variations during strong planetary wave activity in the mesopause region derived from meteor radar observations, *J. Atmos. Sol. Terr. Phys.*, 74, 55–63.
- Takahashi, H., T. Nakamura, T. Tsuda, R. A. Buriti, and D. Gobbi (2002), First measurement of atmospheric density and pressure by meteor diffusion coefficient and airglow OH temperature in the mesopause region, *Geophys. Res. Lett.*, 29(8), 1165, doi:10.1029/2001GL014101.
- Temmer, M., B. Vršnak, and A. M. Veronig (2007), Periodic appearance of coronal holes and the related variation of solar wind parameters, *Sol. Phys.*, 241, 371–383.
- Thayer, J. P., J. Lei, J. M. Forbes, E. K. Sutton, and R. S. Nerem (2008), Thermospheric density oscillations due to periodic solar wind high-speed streams, *J. Geophys. Res.*, 113, A06307, doi:10.1029/2008JA013190.
- Torrence, C., and G. P. Compo (1998), A practical guide to wavelet analysis, *Bull. Am. Meteorol. Soc.*, 79, 61–78.
- Tulasi Ram, S., J. Lei, S.-Y. Su, C. H. Liu, C. H. Lin, and W. S. Chen (2010), Dayside ionospheric response to recurrent geomagnetic activity during the extreme solar minimum of 2008, *Geophys. Res. Lett.*, 37, L02101, doi:10.1029/2009GL041038.
- Xu, J., W. Wang, S. Zhang, X. Liu, and W. Yuan (2015), Multiday thermospheric density oscillations associated with variations in solar radiation and geomagnetic activity, *J. Geophys. Res. Space Physics*, 120, 3829–3846, doi:10.1002/2014JA020830.
- Yi, W., X. Xue, J. Chen, X. Dou, T. Chen, and N. Li (2016), Estimation of mesopause temperatures at low latitudes using the Kunming meteor radar, *Radio Sci.*, 51, 130–141, doi:10.1002/2015RS005722.
- Younger, J. P., C. S. Lee, I. M. Reid, R. A. Vincent, Y. H. Kim, and D. J. Murphy (2014), The effects of deionization processes on meteor radar diffusion coefficients below 90 km, *J. Geophys. Res. Atmos.*, 119, 10,027–10,043, doi:10.1002/2014JD0217.
- Yuan, T., Y. Zhang, X. Cai, C.-Y. She, and L. J. Paxton (2015), Impacts of CME induced geomagnetic storms on the midlatitude mesosphere and lower thermosphere observed by a sodium lidar and TIMED/GUVI, *Geophys. Res. Lett.*, 42, 7295–7302, doi:10.1002/2015GL064860.